

# A MODEL FOR THE ANALYSIS OF CERAMIC FLOORING INTEGRITY

**Application to the study of cracking in tiles**

**Francisco García Olmos**

Technical Architect. Spain

## **ABSTRACT**

One form of damage long observed in ceramic floorings, which unfortunately is still recurring, has been cracking of the floor tiling surface. This malfunction is related to tile installation on layers of mortar that, in turn, rest on layers of sand or gravel. Various studies have described this type of defect and have proposed solutions to eradicate or at least to reduce such effects. In this presentation, apart from addressing the subject in depth, as it is a recurring issue, it is sought to provide a theoretical explanation to the problem with a view to providing better criteria when it comes to taking decisions on the design or construction of ceramic floorings, with sufficient assurance of stability over time. A model is proposed for the analysis of curving in flooring, in addition to a study of the stresses to be withstood by the tiles and a reflection on the importance of the thickness of the mortar layer. At the same time, certain considerations are set out on the "buckling" of sections of tiling as a potential problem deriving from the same source.

## 1. THE PROBLEM

An already classic malfunction in ceramic floorings is the cracking of tiling in fracture lines that, in an apparently random distribution, divide the floor surface into variously shaped polygonal fractions. These correspond to cases of tiles installed on layers of cement mortar, which "float" on beds of sand or gravel. Figure 1 shows one of the forms of tile installation at issue in this study. References are also available on the appearance of these defects in floors on screeds laid on insulations and thick-bed or thin-bed tile fixing, and on screeds of "fluidised" mortar and thin-bed tile installation.



Figure 1. Installation of flooring on gravel and a mortar layer.

This type of failure has been extensively described in the literature by several authors, such as Porcar<sup>1</sup>, Viebig and Porcar<sup>2</sup>, Puce<sup>3</sup> and the author of this paper<sup>4</sup>. All these texts accurately identified cement mortar shrinkage as a driving force behind the problems at issue, and solutions were put forward for prevention.

The observation that has not perhaps sufficiently come across has been the resulting curvature of the floor tiling surface in these cases. This can be clearly observed in the photograph in Figure 2.

The play of light reflections coming from the back clearly highlights the convex parts of the floor tiling.

<sup>1</sup> Defectos y disfunciones en alicatados y solados. J.L. Porcar. Junio 2005.

<sup>2</sup> Disfunciones en acabados de edificios. Pavimentos y revestimientos cerámicos. Jornadas de Debate y Reflexión sobre la aplicación de la L.O.E. J. Viebig y J.L. Porcar.

<sup>3</sup> L.Puce. Boletín del Colegio de Aparejadores y Arquitectos Técnicos de Murcia. December 2002.

<sup>4</sup> Fisuración de pavimentos cerámicos. Una aproximación experimental al problema. F. García BICCE. April 1996.

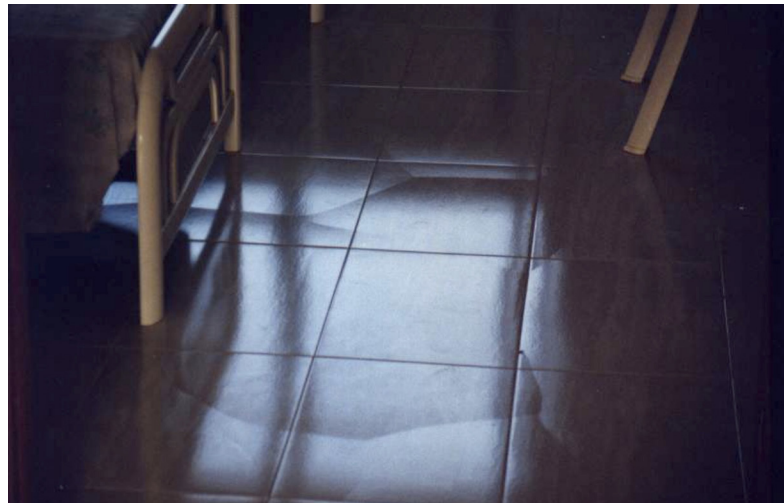


*Figure 2. A good graphic expression of the problem of cracking in flooring.  
Home in Cabezo de Torres. Murcia.*

Other studies<sup>5</sup> have, however, focused directly on the general curvature of the system with lifting in the middle of the section and dropping at the perimeter, a problem that is addressed, in a complementary way, in this study.

The cracking defects mentioned have been evidenced, with relative frequency, in stoneware tile floorings like the one shown in the Figure 2. However, in periods when so-called "small tile slabs" were used, similarly damaged floors were observed. It is striking that this type of problems has even occurred in floorings agglomerated with synthetic resins, indicating that this anomaly is not exclusive to ceramic tiles but rather stems from uniting, in a single system, thin rigid tiles with cement mortars. The photograph in Figure 3 shows a marble dust agglomerate flooring.

Generally, in the inspections conducted, the tiles displayed relatively good bonding to the mortar, mortar layer thickness was about 5 cm, and the mortar layers exhibited a certain hardness when they were drilled.

The evolution over time of such damage suggests the progressive differential deformation of the system constituents, deformation being involved that can stem from well-known processes in the tile and especially in the cement mortar.

Basically, shrinkage of the Portland cement mortar is deemed the principal driver of the process and is generally treated as such in the literature surveyed. However, the dimensional alterations of the ceramic tile, based on expansion/shrinkage owing to moisture or thermal effects, could, depending on their positive or negative sign, contribute to increasing or relieving the process.

<sup>5</sup> Descubriendo razones para el abombamiento. Ingo Grollmisch. Fliesen und Platten.



Figure 3. Marble agglomerate flooring with synthetic resins.

It lies beyond the scope of this study to analyse in detail the cement mortar shrinkage process, but it must be taken into account that a material is involved that is applied "fresh" and that, if it is not allowed to mature sufficiently, the slab shrinkage or shortening resulting from mortar curing is going to have its effect on the system.

With a view to having tools that provide some idea of the mechanical workings of these processes and circumventing the irregular conditions in preparing these floorings, such as possible variations in thickness, non-uniformity in the proportioned quantities, etc., a theoretical study is set out in order to, on the one hand, establish the role of the key parameters and, on the other, to evaluate the possibility that a given situation might result in tile cracking, eventually, buckling of the floor tiling.

## 2. CURVING AS A RESULT OF DIFFERENTIAL INTERLAYER BEHAVIOUR

Surface curving is, in principle, a relatively common phenomenon when the layers making up a system display different behaviour from a dimensional viewpoint. It suffices simply to observe the concave slabs of dry clay at the bottom of what was once a pool, in order to attribute their curvature to the difference in moisture between the different layers.

One only needs to stick a sheet of paper, with a glue that moistens the paper, on a piece of dry cardboard and wait a few minutes to begin to see how the assembly starts curving. Repeating the process on the other side of the cardboard then brings things back into place.

In the case of the tiling on layers of cement mortar, mortar shrinkage<sup>6</sup> is the main driver of the system's curvature. The explanation of this curving mechanism is addressed in Figure 4.

<sup>6</sup> The possible dimensional change in the ceramic tile is not mentioned here, as it is considered to be of very little significance. However, if this is to be included, its unit strain can be added to that of the mortar (with a positive sign in the case of expansion). Mathematically, the origin of the deformation is immaterial, as the relative movements between the two materials are involved.

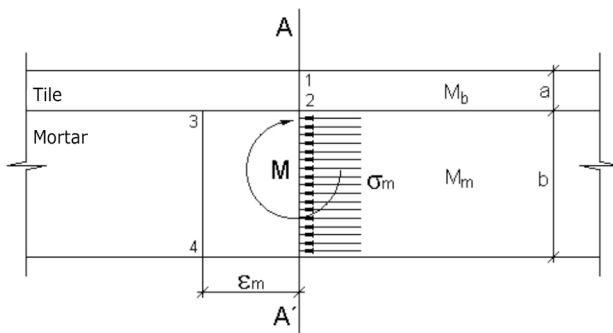


Figure 4. Static starting situation of a floor tiling plane.

This scheme illustrates the situation of a cross-section A-A', in a tile floor on a mortar layer. The tile cross-section on A-A' would be in position 1-2; however, the mortar that, in its shrinkage movement " $\varepsilon_m$ ", tried to reach line 3-4 would cause stress " $\sigma_m$ ", if this displacement were prevented.

$$\sigma_m = \varepsilon_m M_m \quad (1)$$

$M_m$  represents the mortar modulus of deformation here<sup>7</sup>.

This action subjects the tiling section to a bending moment "M", whose magnitude it will be attempted to quantify further below. However, it will already be understood that its direction is such as to cause convexity of the assembly, in the mathematical approach of the term, i.e. viewed from the infinity of an assumed y-axis.

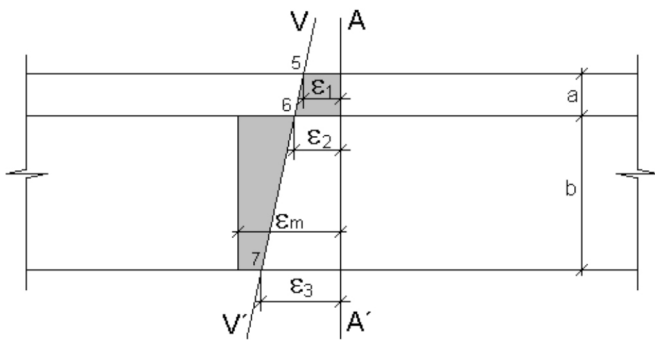


Figure 5. Stresses in the section after the static equilibrium.

Figure 5 illustrates the stressing of the section once the corresponding internal equilibrium has been established. Here the AA' plane has shifted to position VV'. The expected movement of the mortar did not fully take place, producing a certain stress in the mortar and in the tile. Schematically, the magnitudes of these stresses are shown as shaded areas: tension in the mortar and compression in the tile, in this particular case.

<sup>7</sup> The term "moduli of deformation  $M_d$ " is used here instead of "moduli of elasticity E", as prolonged stresses in time are involved, as a result of which the fatigue phenomena, particularly in the mortar, are considerable.

The stresses, at the individual points 5, 6, and 7, can be determined provided the unit displacements " $\varepsilon_1$ ", " $\varepsilon_2$ " and " $\varepsilon_3$ ". are known. These displacements will, therefore, be the unknowns it will be attempted to determine next.

Making the classical assumption of the strength of materials, the static equilibrium of this system of forces can be studied, applied to a section, assuming the tiling to be a continuous system<sup>8</sup> in a slice of unit width.

The following conditions were established:

a) equilibrium of forces that gives rise to the following equation:

$$aM_b\varepsilon_1 + (aM_b + bM_m)\varepsilon_2 + bM_m\varepsilon_3 = 2\varepsilon_m M_m b \quad (2)$$

b) equilibrium of moments:

$$2a^2M_b\varepsilon_1 + (a^2M_b - b^2M_m)\varepsilon_2 - 2b^2M_m\varepsilon_3 = 3\varepsilon_m M_m b^2 \quad (3)$$

c) linearity condition of points 5, 6, and 7:

$$b\varepsilon_1 - (a + b)\varepsilon_2 + a\varepsilon_3 = 0 \quad (4)$$

Arranged in matrix form:

$$\begin{bmatrix} aM_b & aM_b + bM_m & bM_m \\ 2a^2M_b & (a^2M_b - b^2M_m) & -2b^2M_m \\ b & -(a + b) & a \end{bmatrix} * \begin{bmatrix} \varepsilon_1 \\ \varepsilon_2 \\ \varepsilon_3 \end{bmatrix} = \begin{bmatrix} 2\varepsilon_m M_m b \\ 3\varepsilon_m M_m b^2 \\ 0 \end{bmatrix} \quad (5)$$

Note: At the end of this paper, the annotation is detailed in Annex 1 and the deduction of these formulas is detailed in Annex 2, section 1 expressions (A1, A2, and A3).

As may be observed in the matrix of coefficients, the first matrix consists, exclusively, of the static qualities of the tiling: thicknesses and moduli of deformation, whereas the third matrix is made up of the actions. It is obvious that the second matrix is reserved for the unknowns, in this case the resultant displacements at the points that interest us.

Once the unit strains " $\varepsilon_1$ ", " $\varepsilon_2$ " and " $\varepsilon_3$ " are available, the corresponding stresses can be determined.

<sup>8</sup> The influence of tile-to-tile joints is not considered here, as butted tiles are usually involved, i.e. without a joint spacing, which are basically subject to compressive stresses.

At 5 the stress will correspond to:

$$\sigma_5 = \varepsilon_1 M_b \quad (6)$$

At point 6 the stress for the tile will be:

$$\sigma_{6b} = \varepsilon_2 M_b \quad (7)$$

At point 6 for mortar:

$$\sigma_{6m} = (\varepsilon_m - \varepsilon_2) M_m \quad (8)$$

At point 7:

$$\sigma_7 = (\varepsilon_m - \varepsilon_3) M_m \quad (9)$$

At the same time, it is also possible to obtain the curvature radius "r" as characteristic deformation index from the following expression:

$$\rho = \frac{a + b}{\varepsilon_3 - \varepsilon_1} \quad (10)$$

Considering this tensional outlook, from the viewpoint of the stresses that the mortar, as most vulnerable element in the system, is subjected to, it may be observed that, in general terms, the curvature produces the greatest stress in the fibres close to the tile, whereas the fibres that are farther removed become compressed.

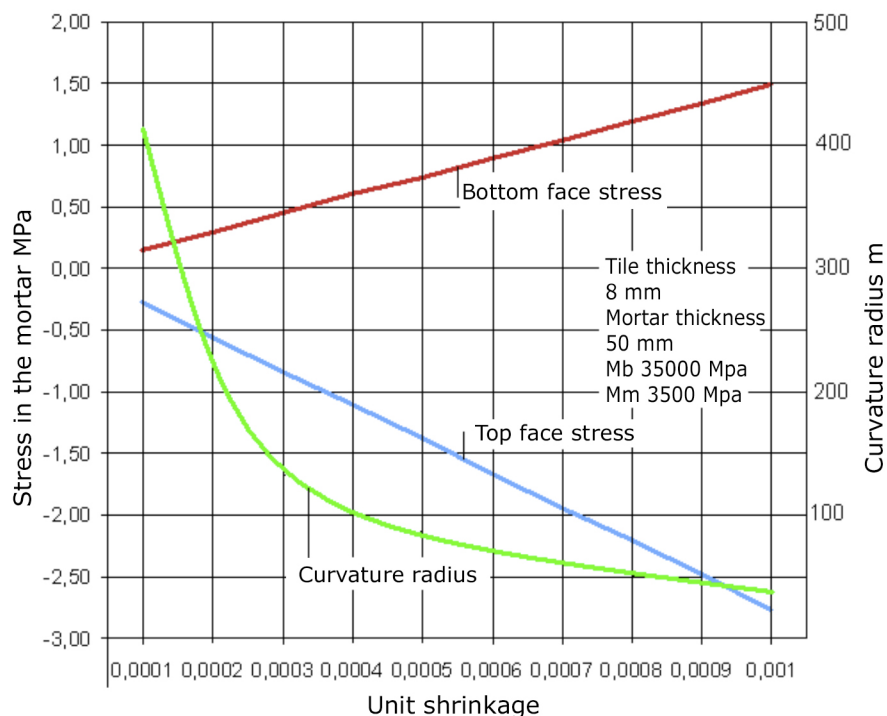


Figure 6. Relationship between unit shrinkage and stressing of the mortar at its two faces.

The example in Figure 6 shows the variation of the stresses in the mortar and of the curvature radius of the assembly when a system is subjected to a growing unit shrinkage, " $\varepsilon$ ". The increase in top surface stresses, under tension, is greater than the bottom surface under compression (the slope is greater). The linear growth of the stresses may be observed with relation to the increase in unit shrinkage.

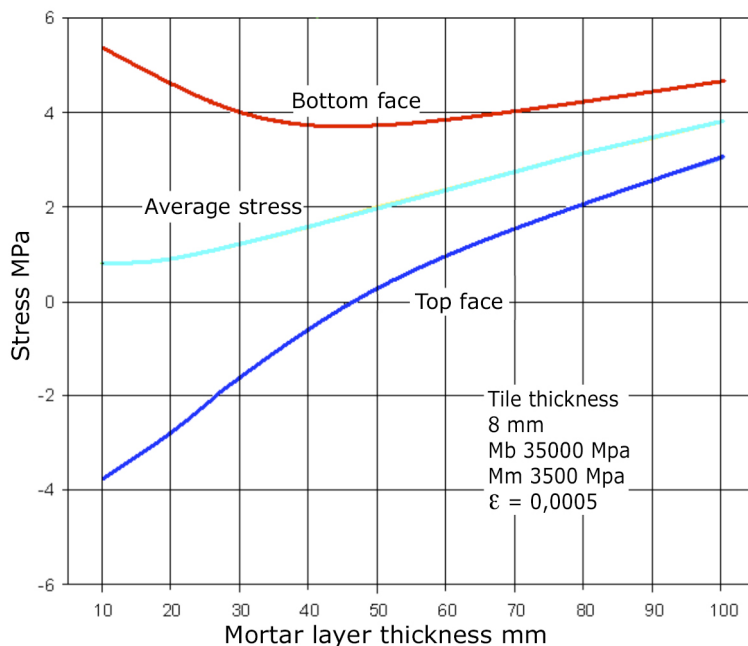


Figure 7. Example of stressing of a tile as a function of screed thickness.

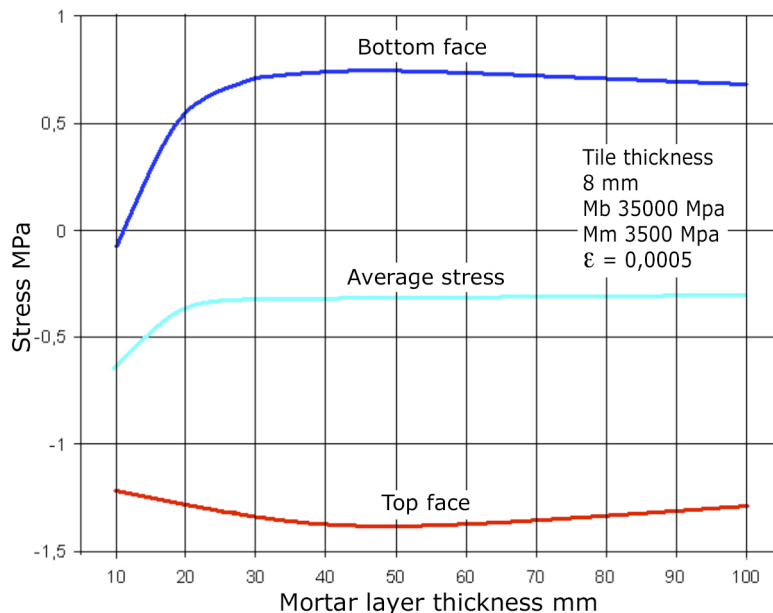


Figure 8. Example of stressing of the mortar as a function of mortar layer thickness.

Figures 7 and 8 show an example of stressing of the tile and of the mortar, respectively. While the average stress in the tile follows a rising path as mortar thickness increases, as its section remains constant, that of the mortar tends to stabilise, in this case, starting at a thickness of 25 mm.

### 3. OBSTACLES FOR THE CURVING AND FLAT SITUATION OF THE FLOORING

Floor tiling can be prevented from curving because of various obstacles or circumstances, which do not allow any or only allow partial curving. These can be divided into two groups: those that can somehow be evaluated (which could be called "Type A") and those that are hard to evaluate ("Type B").

The action of the own weight belongs to the first group, this being a known parameter that can be readily evaluated as a function of the specific weights and respective thicknesses of the elements making up the flooring.

The second group involves other circumstances, such as the following: edge effects resulting from embedding (perimeters without movement joints with mortar stuck to the walls and/or constraints from wall tiling or skirting), connections between the mortar and the base substrate, heavy furniture, sanitary appliances, etc. These circumstances must be taken into account in each particular case, especially in small sections where their effect can be decisive in keeping the tiling flat as set out further below.

In accordance with the considerations noted above, floor tiling can either curve or remain flat.

Curvature or buckling involves conversion of the tiling into a slab supported at its edges or even at its corners, as a very low "sail vault" exposed to fracture as a result of the stress to which it is subjected, as described in the work of Peter Stemmermann<sup>9</sup>, on fracture in buckled stone floorings. These fracture conditions are not analysed in this study.

The fact that a tiling remains flat, owing to constraint by obstacles, does not mean that the system shrinkage and stressing process will disappear, though it introduces changes with respect to the curving position, in the stress distribution in the tiling section as Figure 9 seeks to illustrate.

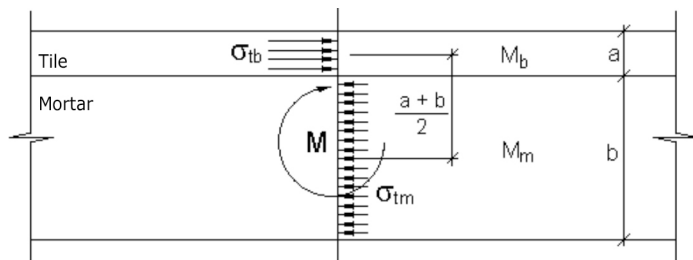


Figure 9. Representation of the tensional state of tiling in a flat situation.

<sup>9</sup> Natural stone technique. Fliesen und Platten 9/2001.

In this case, the stresses of the mortar and the tile remain uniform throughout their section. The three equations of the system (5) are reduced to the first with the section without rotation.

In this case:

$$aM_b\varepsilon_1 + bM_m\varepsilon_1 = \varepsilon_m M_m b \quad (11)$$

The only unknown is the unit shrinkage of the assembly " $\varepsilon_1$ ", the value of which can be calculated as:

$$\varepsilon_1 = \frac{\varepsilon_m M_m b}{M_b a + M_m b} \quad (12)$$

and, consequently, the work stress of the mortar and the tile can be respectively determined from:

$$\sigma_{tm} = (\varepsilon_m - \varepsilon_1) M_m \quad (13)$$

$$\sigma_{tb} = \varepsilon_1 M_b \quad (14)$$

The moment to which this tensional state subjects the section is made up of the pair consisting of the stress resultants of the tile (compression) and the mortar (tension), the arm of which is half the total edge:

$$M = \sigma_{tm} b \frac{a + b}{2} \quad (15)$$

This is the moment that would curve the system if it were released from the corresponding constraints to the curving.

#### 4. INFLUENCE OF THE OWN WEIGHT

In regard to the consideration of the own weight as an obstacle to curvature, Ingo Grollmisch, in his study cited previously, establishes the confrontation of the deflections owing to the curving and to the hypothetical deformation generated by the own weight in order to evaluate the potential buckling.

In accordance with this approach, the expression that determines the deflection owing to the two actions is:

$$f_x = \frac{1}{EI} \left[ \frac{5}{384} (a + b) \gamma l^4 - \frac{1}{16} (a + b) \sigma_{tm} b l^2 \right] \quad (16)$$

See Annex 2, Section 2, expression (A4).

In order to cancel out the deflection and keep the flooring flat, the following must be obeyed:

$$\frac{5}{384}(a+b)\gamma.l^4 = \frac{1}{16}(a+b)\sigma_{tm}b.l^2$$

which gives:

$$\sigma_{tm} = \frac{5\gamma.l^2}{24b} \quad (17)$$

This means that the mortar working stress " $\sigma_{tm}$ " required to lift and curve a flooring with a span " $l$ " and average specific weight " $\gamma$ ", for a screed thickness " $b$ ", can be determined. The lower that stress, the easier will buckling take place.

Figure 10 shows a graph, for different screed thicknesses, of mortar working stress as a function of the span of the section considered.

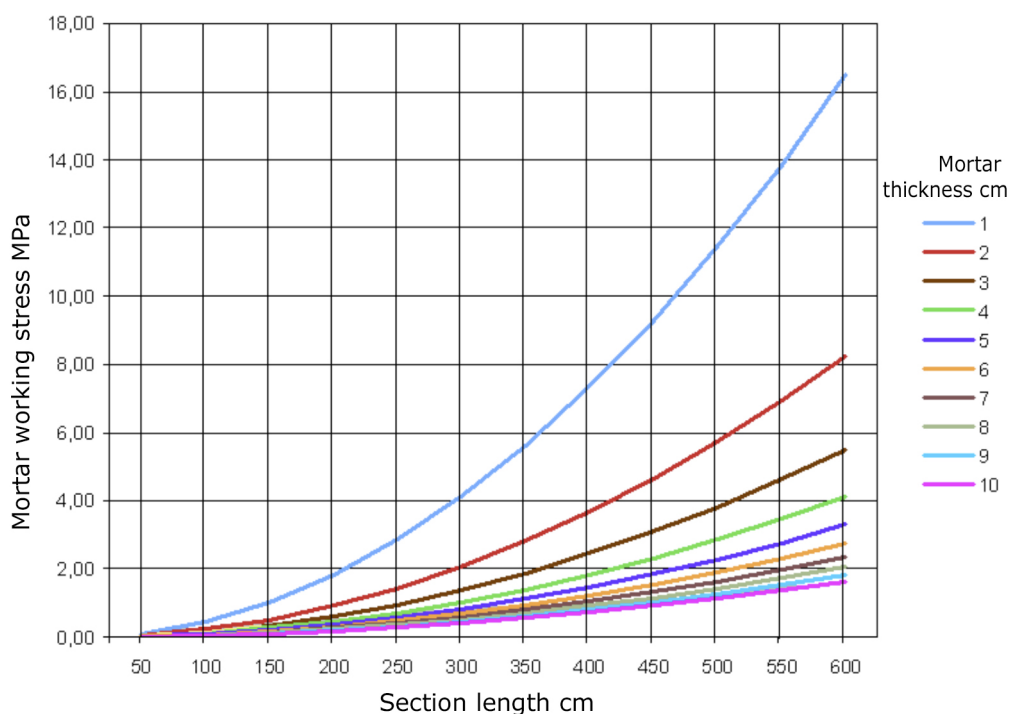


Figure 10. Relationship between the size of a section and the mortar working stress required to overcome the own weight (assuming an average specific weight of 2,2 g/cm<sup>3</sup>).

The result is that though the required working stress of the cement mortar is relatively small for short sections (smaller than a metre, for example), it takes on a certain magnitude as the size increases, therefore making buckling easier.

Similarly, mortar screed thickness plays an important role. particularly when the thickness is small. The curves corresponding to these thicknesses are clearly separated from the rest, as may be observed in the graph. Greater mortar thickness leads to greater ease for buckling.

## 5. A CRUCIAL INCIDENT. MORTAR CRACKING. INTER-CRACK SPACING

The element that most tends to fail on exposure to stresses in the tiling system is undoubtedly the mortar. Exceeding the fracture stress, with the ensuing cracking of the mortar, evidently weakens the stiffness of the assembly.

The alteration produced by cracks in the mortar leads to a substantial and decisive change in the mechanical situation of the system. On the one hand, it modifies the starting tensional state, assumed uniform throughout the system, and, more importantly, points are created at which the tile is the only remaining element of continuity.

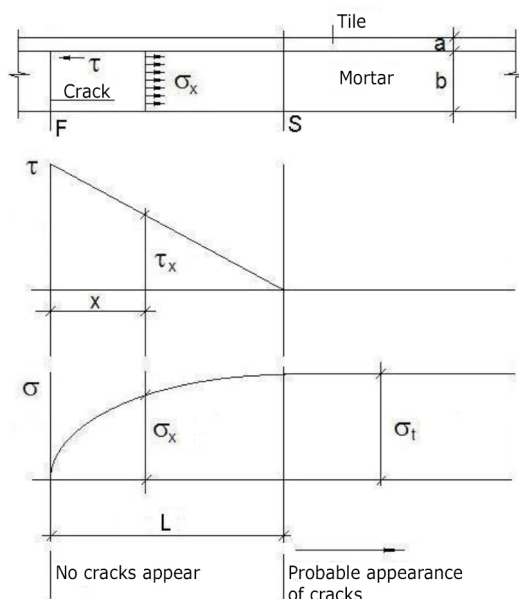


Figure 11. Tensional distribution of " $\sigma$ " and " $\tau$ " from the existence of a crack in mortar.

If a flat system is assumed, the possible spacing between cracks in mortar layers can be studied<sup>10</sup> by establishing the equilibrium of the forces that exist after the appearance of the first crack. The schemes in Figure 11 attempt to capture the tensional situation in the mortar, in the case of cracking.

Thus, in a system subjected to a constant stress in the mortar, when this stress reaches failure " $\sigma_t$ ", a crack develops, for example in plane "F", and the normal stress at that crack face then disappears. The value " $\sigma_x$ " then begins to grow progressively until it reaches the value " $\sigma_t$ " again in the plane "S" where another crack can appear again. Concurrently, at the crack–tile line, grazing stresses " $\tau$ " appear that attempt to offset the disappearance of stress " $\sigma$ ", which are cancelled out in "S".

<sup>10</sup> Albert Joisel. Fisuras y Grietas en Morteros y Hormigones.

Assuming a linear distribution of " $\tau$ ", the equilibrium of forces at the height of "S" can be established:

$$b\sigma_t = \frac{\tau}{2}L \quad (18)$$

" $\tau$ " depends on the tile/mortar adhesive strength that the value of " $\sigma_t$ " will, at most, reach in the case of an extraordinary bond strength. With an average adhesive strength, " $\tau$ " can take on values of " $\sigma_t/3$ " or " $\sigma_t/4$ ", these being values more consistent with reality.

If the ratio " $\sigma_t/\tau$ ", is termed " $\beta$ " the previous expression becomes

$$b\sigma_t = \frac{\sigma_t}{2\beta}L \quad \text{and therefore} \quad L = 2\beta b \quad (19)$$

This means that the cracks will be separated by a minimum spacing of " $2\beta$ " times the mortar thickness. From that distance, another crack parallel to the first can open up because the stress again becomes fracture stress. A crack at "F'" symmetrical to the plane "F" on the "S" axis would constitute the maximum possible inter-crack spacing, keeping the stress " $\sigma_t$ ". in the centre. To both sides of "S", the stress would decrease. This maximum spacing is, therefore " $4\beta$ " times the mortar thickness, as illustrated in Figure 12.

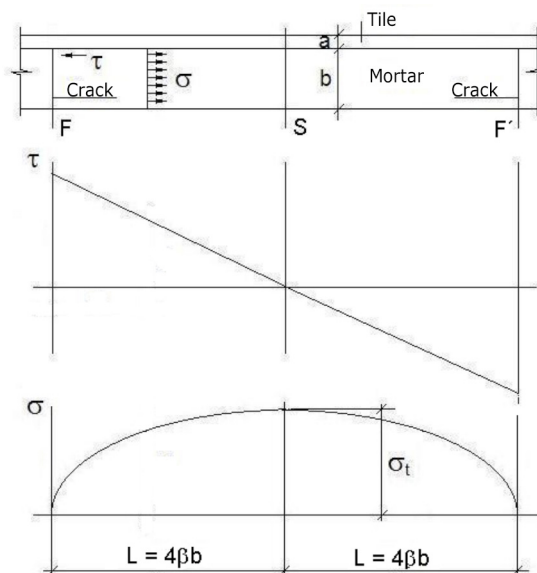


Figure 12. Maximum inter-crack spacing situation..

In short, the cracks in the mortar would theoretically open up at distances between  $2\beta b$  and  $4\beta b$ :

$$2\beta b \leq 2L \leq 4\beta b \quad (20)$$

For example: for a mortar thickness of 5 cm and  $\beta = 3$  the spacing between parallel cracks would be between 30 cm and 60 cm.

## 6. CRACK DISTRIBUTION IN THE FLOOR PLANE

It should be borne in mind, first, that a section of curved tiling, subject to service loads, can fracture as described above. The study of such fracture lies beyond this study and it can be approached, perhaps, by means of the theory of fracture lines. In that case, the crack pattern in the plane would be quite different from that addressed here, but it would not be difficult to find this in practice. This type of malfunction typically features fractures that divide the sections into large fragments, following the lines of maximum bending moment. Here, however, cracks caused by shrinkage phenomena are involved and, as such, they exhibit a very different trend in their arrangement.

Viewed from the surface, the shrinkage crack pattern can adopt different forms. Certain publications<sup>11</sup> have shown that the tensional state of a slab of concrete or mortar leads to the formation of right angles between cracks.

In other cases<sup>12</sup>, a tendency has been recognised for trios of cracks to appear, arranged at angles of 120°. The photographs in Figure 13 depict this cracking morphology. The crack lines have been marked to enable this to be clearly observed. This materialisation was, however, also quite visible in the photograph in Figure 2. On other occasions, cracks have been described that start out from the corners of partitions or walls.



Figure 13. Cracks tending to form angles of 120°.

These forms of fragmentation of the plane have a theoretical foundation, if the stressing of a slab of mortar is analysed. The schematic illustration in Figure 14 attempts to explain, in a very simplified form, these crack dynamics.

The multidirectional state of the stress at any point P in the slab of mortar can be summed up in the corresponding resultants of the vertical and horizontal components, a) and b) in Figure 14. The formation of a crack "F", let us say vertical, which passes through that point, c) of the figure, would cancel out the horizontal components of the

<sup>11</sup> Albert Joisel. Fisuras y Grietas en Morteros y Hormigones.

<sup>12</sup> Manual de pavimentos industriales. IECA.

system on both sides of that crack. The mortar would only be subject to stresses with the vertical components and would cause the crack  $F'$  to appear on one or on both sides of  $F$ . This would explain the appearance of right-angle cracks.

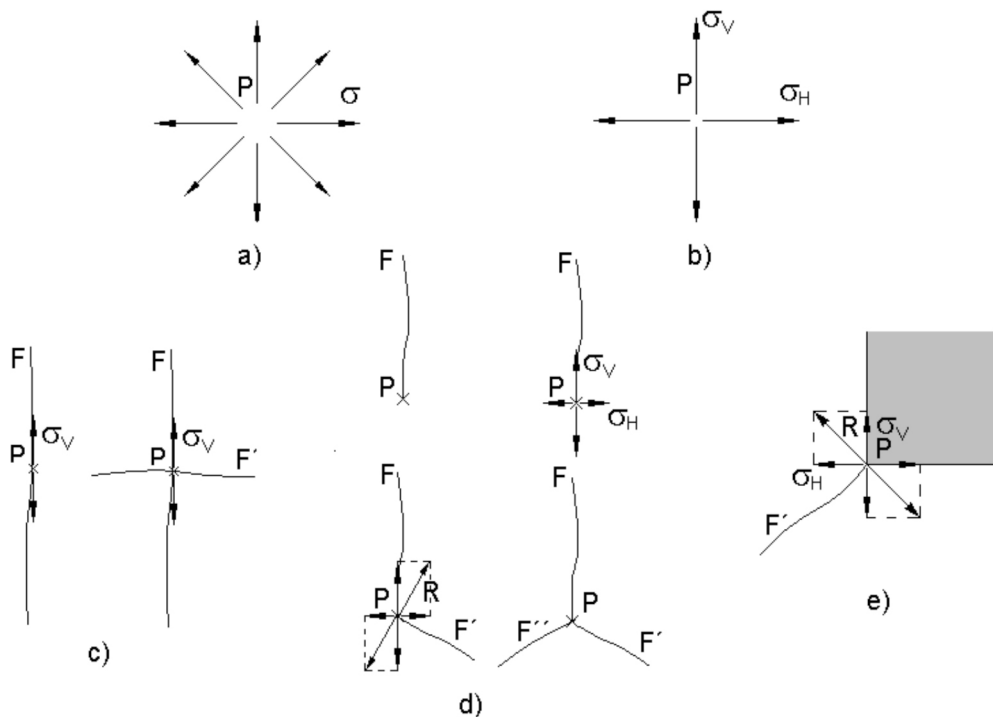


Figure 14. Simplified explanation of the appearance of different crack morphologies.

In contrast, if "P" is considered at the end of a crack that is forming, as illustrated in d) of Figure 14, the horizontal stress components only cancel out in the top part of the horizontal at "P", so that they could remain in the middle of the initial stress. The maximum stress "R" around "P" would be reached with the composition of these decreased horizontal components and corresponding vertical components. Crack  $F'$  opens up normal to "R" with an angle similar to  $120^\circ$  (about  $117^\circ$ ). The overview is completed with crack  $F''$  as a result of the formation of a corner between  $F$  and  $F'$ .

As it is attempted to explain in e), the cracks that set out from a corner follow the bisector of the obtuse angle that the corner itself forms in the slab of mortar.

These three forms of cracking: at a right angle, at an angle of about  $120^\circ$ , and setting out from a corner, have been observed in damaged ceramic floorings as described here. It may be noted, however, that there is no clear or regular modulation.

Apart from other considerations, in certain cases, the variability in mortar layer thickness can lead to very irregular crack maps. The photograph in Figure 15 shows the variation in thickness of an extracted mortar layer fragment in a particular case.



Figure 15. Extracted mortar layer fragment of a ceramic tiling.

In short, cracks can end up dividing the tiling plane in portions or sections with apparently fanciful shapes. However, with a view to making the theoretical calculations set out here meaningful, the distances between parallel cracks have been assumed to match those described in the previous section and the stresses to be applied in any direction, in each case extracting ideal slices of unit width with a "characteristic" inter-crack spacing, let us say, of "2 $\beta$ b" to "4 $\beta$ b".

## 7. STATICS OF THE INTER-CRACK STRETCH

As described, shrinkage effects can lead to mortar fracture stress, dividing the agglomerate layer into a series of fragments separated by crack lines under the tiling, these being fragments that tend to take on the form of quasi-spherical caps.

In this curving movement the mortar encounters the constraint of the tile, resulting in the appearance of the corresponding moment as an "embedding". The scheme in Figure 16 illustrates this situation. The tile section on top of the crack undergoes a moment bending "Me", which subjects the tile to simple bending, with tension at its bottom surface and compression at its proper surface<sup>13</sup>.

<sup>13</sup> This compression situation at the tile proper surface explains why, in the case of fracture, the crack opening is minimum and can often only be seen "against the light". Such compression leads, with relative frequency, to "chipping" of the edges.

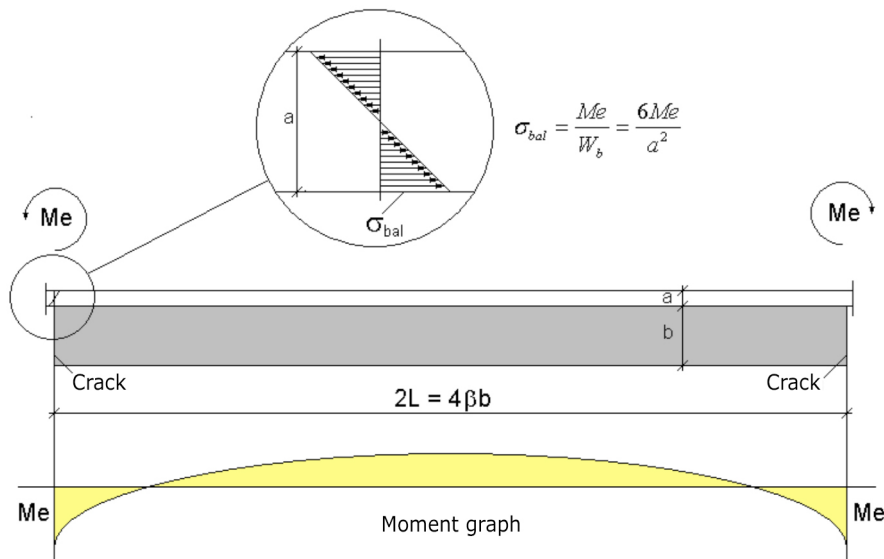


Figure 16. Moment at the ends of the stretch that the tiles need to withstand in the most unfavourable situation.

The moment "Me" can be separately evaluated for the shrinkage effects as:

$$Me_1 = \frac{2\sigma_t b}{3} \left[ \frac{a+b}{2} \right] \quad (21)$$

See Annex 2 Section 3.1 Expression (A5).

And, albeit of little magnitude, the counter action caused by the own weight:

$$Me_2 = (a+b) \cdot \gamma \frac{L^2}{3} \quad (22)$$

See Annex 2 Section 3.2 Expression (A7).

These moments give rise to the corresponding stresses, set out below.

The stress deriving from tile bending stress in the stretch on the cracks owing to the shrinkage would be:

$$\sigma_{bal1} = 2\sigma_t b \frac{a+b}{a^2} \quad (23)$$

See Annex 2 Section 3.1 Expression (A6).

The stress corresponding to the own weight:

$$\sigma_{bal2} = \frac{2(a+b)}{a^2} \gamma \cdot L^2 \quad (24)$$

See Annex 2 Section 3.2 Expression (A8).

Which would yield:

$$\sigma_{bal} = 2 \frac{a+b}{a^2} (\sigma_t b - \gamma \cdot L^2) \quad (25)$$

Consequently, the stress to which the tile could be subjected to in the most unfavourable case, in a given stretch of tiling, depends fundamentally on the working stress that the mortar can reach as a result of the shrinkage process, represented at the bound, by its fracture stress. The own weight of the system contributes to slightly minimising this stress.

As the mortar fracture stress cannot be exceeded, its value can be very useful in relation to the working of the mechanism that produces tile cracking.

Solving " $\sigma_t$ " in expression (25), one obtains:

$$\sigma_t = \sigma_{bal} \frac{a^2}{2b(a+b)} + \frac{\gamma \cdot L^2}{b} \quad (26)$$

The calculated value of " $\sigma_t$ " is therefore the minimum fracture stress that the mortar needs to reach to crack the tile.

If "L" is assigned the value "6b" ( $\beta=3$ )<sup>14</sup>, for example, this expression is reduced to its most practical form:

$$\sigma_t = \sigma_{bal} \frac{a^2}{2b(a+b)} + 36 \cdot \gamma \cdot b \quad (27)$$

## 8. CRACKING OR BUCKLING OF THE FLOORING

The expression (27) represents the value of the fracture stress required to crack the tile. Expression (12) established the working stress " $\sigma_{tm}$ " of the mortar, which, taken to the bound as fracture stress, is needed to buckle a section of size "l" (here designated " $\sigma'_t$ ").

$$\sigma'_t = \frac{5\gamma \cdot l^2}{24b} \quad (28)$$

Both fracture stress values, understood as the bounds of the mortar working stress, can be graphically illustrated, as in Figure 16, in which their respective developments can

<sup>14</sup> Fixing this value has a relative influence, given the little influence on the final result of the own weight for the small-sized fragments shown in section 4.

be conveniently examined for the different mortar thicknesses. However, the interpretation of these curves needs to take into account the following points:

- The red curve that represents the evolution of " $\sigma_t$ " is no longer meaningful when the system curves, so that the segment on the left of the cut-off point "E" is dashed. It would depend on the existence of obstacles of type B, which prevented curving, in order to be useful.
- The blue curve, which represents the values of " $\sigma'_t$ ", is no longer applicable when the mortar has cracked. However, in the graph it is plotted in its entirety without any observation because, for the tile to crack, the mortar must crack so that, to the right of "E", if the mortar working stress exceeds the blue line without reaching the fracture stress, buckling will take place provided there are no B-type obstacles.
- As it was noted previously, tile cracking conditions in a buckled system are subject to variables that are not considered in this study.

The fundamental usefulness of this type of graph, apart from more complex interpretations, is in providing information on the "safety margin", which lies beneath the two curves.

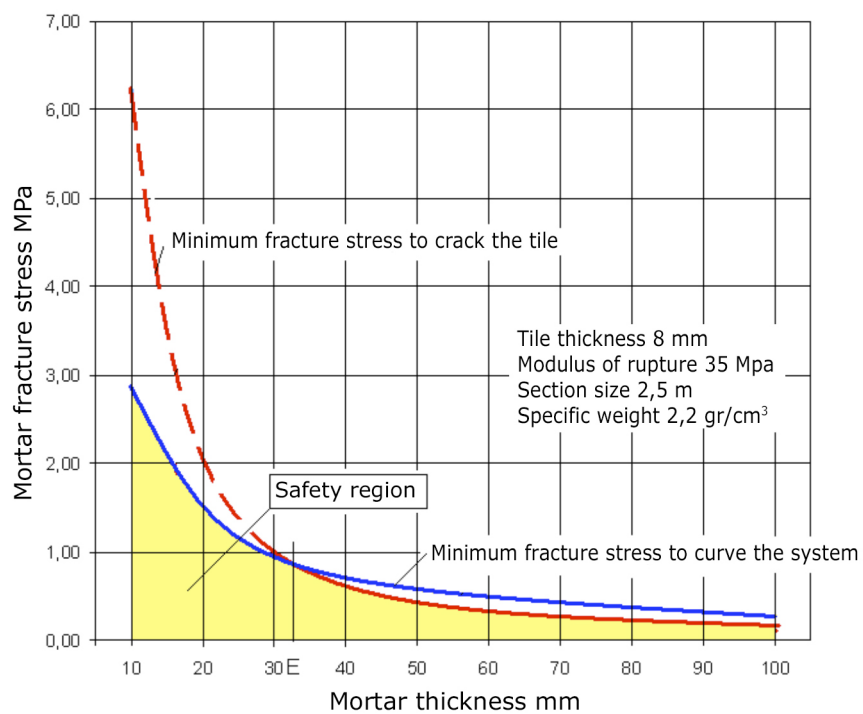


Figure 17. Curves of fracture stress required for buckling and cracking the tiles as a function of mortar thickness.

These relative positions of the curves vary. The blue curve rises when the section size increases and descends when it decreases. The curves for different section sizes are plotted in Figure 18. As may be observed, the curve corresponding to 4 m, in the

range considered, remains in its entirety above the curve of the stresses required for tile fracture because surface curving is more difficult, owing to the repercussion of the own weight.

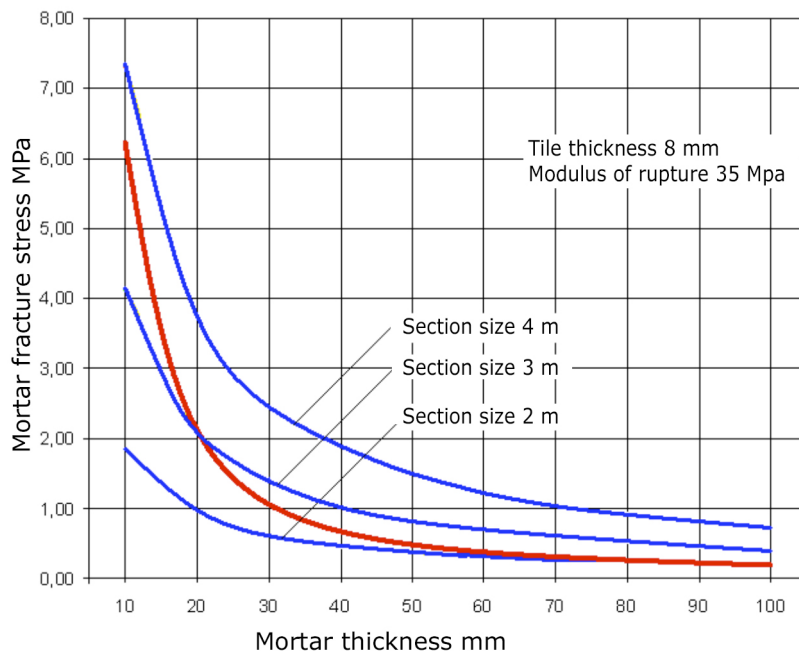


Figure 18. Relationship between the curves of the mortar fracture stress required for buckling and cracking the tiles for several section sizes.

In contrast, the curve corresponding to the 2 m section length remains underneath. Surface curving is verified more easily. This explains the relatively ready buckling of the fragments resulting from tile cracking.

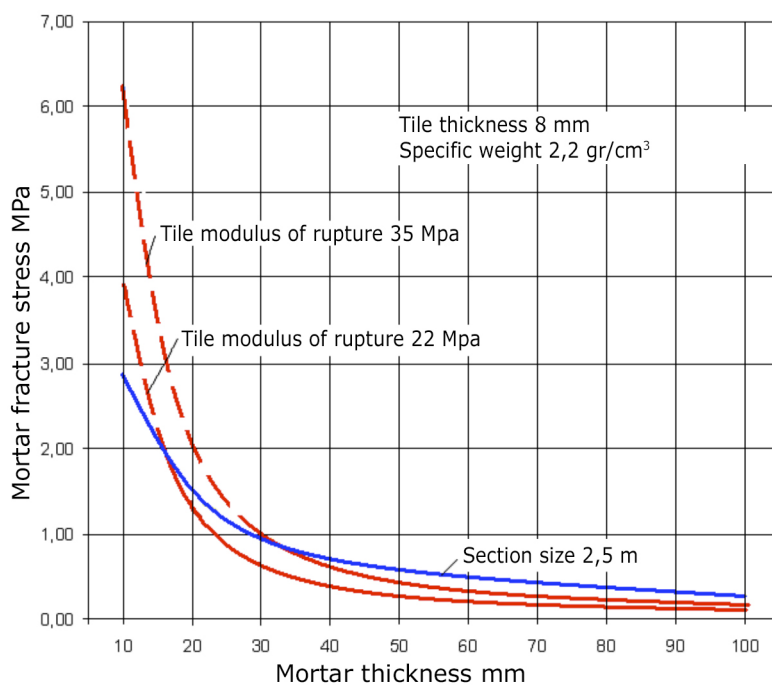


Figure 19. Influence of tile bending strength in relation to the mortar fracture stress required for buckling and cracking of the tiles.

The curves relating to the stress required for the buckling and cracking of tiles with two different moduli of rupture and a section size of 2,5 m are plotted in Figure 19. The curve corresponding to 22 MPa reduces the stresses required for cracking, which highlights the importance of ceramic tile mechanical strength.

## 9. THE MORTAR FRACTURE STRESS/THICKNESS BINOMIAL

It is clear that a powerful means of combatting the materialisation of any tile buckling or cracking processes is keeping the mortar fracture stress below the curves discussed in the previous section. However, the corresponding graphs show that, as screed thickness grows, these curves tend to leave less space beneath the curves to accommodate the fracture stress in that zone. It would therefore appear advisable to keep the mortar thickness within small values, in which the ordinate of the curves is greater.

Expressions (27) and (28) allow one to use the screed strength/thickness binomial to achieve a foreseeably safe situation for the floor tiling.

Example:

Tile modulus of rupture 30 MPa

Tile thickness 10 mm

Specific weight of the flooring 2,2 g/cm<sup>3</sup>

Mortar thickness 50 mm

Section size 3 m

$$\sigma_{tm1} = \sigma_{bal} \frac{a^2}{2b(a+b)} + 36 \cdot \gamma \cdot b = 30 \frac{10^2}{2.50(10+50)} + 36 \cdot 2.2 \cdot 10^{-5} \cdot 50 = 0,54 \text{ MPa}$$

$$\sigma_{tm2} = \frac{5\gamma \cdot l^2}{24b} = \frac{5 \cdot 2.2 \cdot 10^{-5} \cdot 3000^2}{24 \cdot 50} = 0,83 \text{ MPa}$$

If it is considered difficult to obtain a mortar tensile fracture stress below 0,54 MPa, the mortar thickness can be reduced.

Setting a thickness of 20 mm, the new values would be:

$$\sigma_{tm1} = \sigma_{bal} \frac{a^2}{2b(a+b)} + 36 \cdot \gamma \cdot b = 30 \frac{10^2}{2.20(10+20)} + 36 \cdot 2.2 \cdot 10^{-5} \cdot 20 = 2,52 \text{ MPa}$$

$$\sigma_{tm2} = \frac{5\gamma \cdot l^2}{24b} = \frac{5 \cdot 2.2 \cdot 10^{-5} \cdot 3000^2}{24 \cdot 20} = 2,06 \text{ MPa}$$

These last values, above 2 MPa, provide more room to assure that the mortar fracture stress will not reach critical values.

## 10. SYNOPSIS

The following table summarises the influence of the main parameters in tiling buckling and tile cracking processes. Note that these parameters are deemed to be within reasonable values in terms of their usual composition because, if taken to extreme values, the direction of their influence could change.

Parameter	Influence on system buckling	Influence on tile cracking
Mortar shrinkage	Mortar shrinkage is the driver of curvature and, therefore, an essential prerequisite for the buckling. Whether it is a sufficient condition or not will depend on system composition: moduli of deformation, thicknesses, and size of the sections.	The combination of mortar shrinkage with the corresponding modulus of deformation determines, all other parameters being equal, stressing of the entire system and consequently possible tile cracking.
Moduli of deformation	Although in general the moduli of deformation contribute to the stiffness of the system and therefore, counter its deformation as occurs with the tile modulus of deformation, the effect of mortar shrinkage raises the stress in the system with its modulus of deformation and, therefore, contributes to buckling.	Mortars with a high modulus of deformation and high shrinkage constitute the worst scenario for ceramic tile stability.
Tile thickness	Given the little margin within which tile thickness fluctuates, its influence is relative. However, its increase raises the section's moment of inertia and therefore reduces curvature.	The tile working stress in the most demanding section (on top of the mortar cracks) depends, as in any element subjected to simple bending, on its thickness. A slight increase in this parameter significantly reduces the corresponding stress so that, in short, it reinforces the system against tile cracking.
Mortar thickness	The increase in mortar layer thickness contributes significantly to buckling of the flooring, especially in large-sized sections. In very small sizes, a reduction in thickness in turn decreases the curvature radius.	Mortar thickness acts, squared, in the expression that determines the stress to which a tile is subjected, so that its influence is decisive. Control of this parameter can be a very important factor in maintaining tile integrity.
Size of the floor tiling section	The section size has a major influence on tiling buckling. In large sections, the combination span/own weight is unlikely to allow system buckling unless sufficient inertia is available. In contrast, in small sizes, as is the case of floor tiling fragments "between cracks", buckling takes place very easily.	Tile cracking occurs once the general section has been divided into fragments, so that size does not have a direct influence on cracking.
Tile mechanical strength	Given the usual mechanical performance of ceramic tile, the stresses to which tiles are subjected in the buckling process are widely exceeded by the former. Consequently, the strength characteristics of tiles are only of influence to the extent that they are related to the deformation modulus.	This is a fundamental parameter with regard to withstanding the stresses that the bending movement generates in the section "on top of cracks". Together with a sufficient thickness, as a last resort, the tile can "save" the integrity of the tiling.

Mechanical strength of cement mortars	<p>Tiling curvature is not possible unless the mortar is subjected to tensile stress. The use of "lean mortar" with insufficient strength to maintain the consistency of the system is an obvious impediment to avoiding curvature. If the fracture stress does not exceed the value:</p> $\sigma_t = \frac{5\gamma.l^2}{24b}$ <p>section buckling cannot, theoretically, occur.</p>	<p>The damage mechanisms that can ultimately cause cracking in the tile need a certain mortar working stress. If this stress is not reached, these mechanisms cannot work. One of the ways to keep this stress from being reached is to use mortars that will not provide the tensile strength that facilitates such working stress.</p> <p>Provided that the mortar fracture stress does not exceed the value:</p> $\sigma_t = \sigma_{bal} \frac{a^2}{2b(a+b)} + 36.\gamma.b$ <p>tile cracking cannot, theoretically, occur.</p>
---------------------------------------	--	--

Table 1. Summary of the influence of different parameters on buckling and cracking processes in ceramic floorings.

## 11. ADDITIONAL CONSIDERATIONS AND LIMITATIONS IN THE MODEL

In this study, aspects relating to the progress in time of cement mortar setting, hardening, and shrinkage processes have not been considered. Issues therefore remain to be addressed that can be interesting, even though they may perhaps be of little practical relevance, such as the growth of mortar fracture stress once cracking has occurred, provided that the shrinkage process continues.

Another aspect surely of greater interest, not addressed here, is the inclusion of layers of adhesives on top of the screed with the consideration of their characteristics: thickness, deformability, adhesive strength, etc.

Similarly, the role of tile-to-tile joints has not been examined. Note that in all the observed case studies, the tiles were installed with butted joints, which does not prevent the problems studied from occurring in floorings with joint spacings.

## 12. CONCLUSIONS

The construction of ceramic floor tilings by installing the tiles on mortar layers that are prone to undergo shrinkage processes entails a risk for tile integrity and in many cases breaks up the system. This repeated failure has led to a relative loss of recognition of ceramic tile as a lasting, beautiful, and economical element for floorings.

In this study it has been sought to explain, from a theoretical viewpoint, the mechanisms that lead to curving of the system and cracking of the tiles, with a view to identifying the key parameters in the process.

Using the proposed tools it is possible to study the stressing of the system and its curvature, analysing the map of cracks in the flooring and the participation of each parameters in the buckling of the floor tiling and in the cracking of the tiles themselves.

In a first analysis, it may be said that, of all the parameters in the context of the actions, the magnitude of effective mortar shrinkage, which is always difficult to foresee, defines the effective possibilities of the degradation mechanisms, and the origin of the damage processes depends on its control. However, its damage capability depends in turn on the resistance capacity of the assembly.

Within the parameters of the system's "resistance", apart from the logical positive influence of the quality of the tile, mortar strength and especially mortar thickness play a decisive role. Consequently, independently of the actions that could be generated in the assembly, appropriate design of the mortar layer can liberate the system from buckling and the tile from pernicious cracks.

Mortars with low tensile strength and reasonably low thicknesses prevent damage mechanisms from developing sufficient capacity to cause tile break-up as has been described here. However, "lean" cement mortar layers with high thicknesses can break-up the floor tiling.

The Spanish Technological Standard NTE-RSR (1984), despite its antiquity and simplicity, is not misguided in this regard on establishing a mortar thickness limit of 20 mm.

## REFERENCES

- [1] Defectos y disfunciones en alicatados y solados. J.L. Porcar. Junio 2005.
- [2] Disfunciones en acabados de edificios. Pavimentos y revestimientos cerámicos. Jornadas de Debate y Reflexión sobre la aplicación de la L.O.E. J. Viebig y J.L. Porcar.
- [3] Discovering reasons for buckling. Ingo Grollmish. Fliesen und Platten. 08/2005.
- [4] Fallos en los pavimentos cerámicos. L.Puce. Boletín del Colegio de Aparejadores y Arquitectos Técnicos de Murcia. December 2002.
- [5] Fisuración de pavimentos cerámicos. Una aproximación experimental al problema. F. García BICCE. April 1996.
- [6] Fisuras y Grietas en Morteros y Hormigones. Albert Joisel. Editores Técnicos Asociados.
- [7] Norma Tecnológica de la Edificación NTE RSR 1984. Ministerio de Fomento. Spain.
- [8] Stone tile technique. Peter Stemmermann Fliesen und Platten. 09/2005.
- [9] Manual de pavimentos industriales. Instituto Español del Cemento y sus Aplicaciones IECA.

## A MODEL FOR THE ANALYSIS OF CERAMIC FLOORING INTEGRITY

### ANNEX 1. ANNOTATION

#### Terms used

##### Geometry and deformation

a	Tile thickness
b	Mortar thickness
l	Length of a floor tiling section
I	Section moment of inertia
L	Half-length of an inter-crack stretch
M	Bending moment acting in the section owing to shrinkage
Me	Moment to be withstood by the tile
$M_x$	Bending moment acting in a given section
Mb	Tile modulus of deformation
Mm	Mortar modulus of deformation
$W_b$	Tile bending modulus $W_b = a^2/6$
$\beta$	$\sigma/\tau$ ratio
$\gamma$	Average specific weight of the flooring
$\varepsilon_n$	Unit deformation at point n
$\varepsilon_b$	Tile unit deformation
$\varepsilon_m$	Mortar unit deformation
$\Phi_n$	Rotation of the elastica at a point n
$\rho$	Curvature radius
$\sigma_{tm}$	Mortar working stress
$\sigma_{mx}$	Mortar working stress in an abscissa section x
$\sigma_t$	Mortar fracture stress
$\tau$	Bond stress at the end of the stretch
$\tau_x$	Bond stress in an abscissa section x
$\sigma_{bal}$	Tile stress "on top of the crack"

## A MODEL FOR THE ANALYSIS OF CERAMIC FLOORING INTEGRITY

### ANNEX 2. CALCULATION

#### 1. DEDUCTION OF THE EQUATIONS OF EQUILIBRIUM IN A TILING SECTION

- Equilibrium of forces

$$aM_b \left( \frac{\varepsilon_1 + \varepsilon_2}{2} \right) + bM_m \left( \frac{\varepsilon_2 + \varepsilon_3}{2} \right) = \varepsilon_m M_m b$$

Eliminating denominators and simplifying

$$aM_b \varepsilon_1 + (aM_b + bM_m) \varepsilon_2 + bM_m \varepsilon_3 = 2\varepsilon_m M_m b$$

- Equilibrium of moments. Taking moments from the tile–mortar line

$$\frac{a^2 M_b}{2} \varepsilon_1 + \frac{a^2 M_b}{6} (\varepsilon_2 - \varepsilon_1) - \frac{b^2 M_m}{2} \varepsilon_2 - \frac{b^2 M_m}{3} (\varepsilon_3 - \varepsilon_2) = \frac{\varepsilon_m M_m b^2}{2}$$

Eliminating denominators and simplifying

$$2a^2 M_b \varepsilon_1 + (a^2 M_b - b^2 M_m) \varepsilon_2 - 2b^2 M_m \varepsilon_3 = 3\varepsilon_m M_m b^2$$

- Linearity condition of points 5, 6, and 7

$$\frac{\varepsilon_2 - \varepsilon_1}{a} = \frac{\varepsilon_3 - \varepsilon_2}{b}$$

$$b\varepsilon_1 - (a + b)\varepsilon_2 + a\varepsilon_3 = 0$$

Resulting system of equations:

$$aM_b \varepsilon_1 + (aM_b + bM_m) \varepsilon_2 + bM_m \varepsilon_3 = 2\varepsilon_m M_m b \quad (A1)$$

$$2a^2 M_b \varepsilon_1 + (a^2 M_b - b^2 M_m) \varepsilon_2 - 2b^2 M_m \varepsilon_3 = 3\varepsilon_m M_m b^2 \quad (A2)$$

$$b\varepsilon_1 - (a + b)\varepsilon_2 + a\varepsilon_3 = 0 \quad (A3)$$

## 2. DEFLECTIONS OWING TO SHRINKAGE AND THE OWN WEIGHT

The equation of moments of a stretch of tiling made up the two actions would be:

$$M_x = \frac{1}{2}(a+b)\gamma.l.x - \frac{1}{2}(a+b)\gamma.x^2 + M$$

As according to expression (15) in the text:

$$M = \frac{a+b}{2}\sigma_{tm}b$$

$$M_x = \frac{1}{2}(a+b)\gamma.l.x - \frac{1}{2}(a+b)\gamma.x^2 + \frac{1}{2}(a+b)\sigma_{tm}b$$

The expression that determines the rotation in each section:

$$\Phi_x = \frac{1}{EI} \int M x dx = \frac{1}{EI} \left[ \frac{1}{2^2} (a+b)\gamma.l.x^2 - \frac{1}{2.3} (a+b)\gamma.x^3 + \frac{1}{2} (a+b)\sigma_{tm}bx + K \right]$$

For  $x = l/2$   $\Phi = 0$

$$K = -\frac{1}{2^3.3} (a+b)\gamma.l^3 - \frac{1}{2^2} (a+b)\sigma_{tm}b.l$$

Then:

$$\Phi_x = \frac{1}{EI} \left[ \frac{1}{2^2} (a+b)\gamma.l.x^2 - \frac{1}{2.3} (a+b)\gamma.x^3 + \frac{1}{2} (a+b)\sigma_{tm}bx - \frac{1}{2^3.3} (a+b)\gamma.l^3 - \frac{1}{2^2} (a+b)\sigma_{tm}b.l \right]$$

The equation that determines the deflection is:

$$f_x = \frac{1}{EI} \iint M_x dx$$

So that:

$$f_x = \frac{1}{EI} \left[ \frac{1}{2^2.3} (a+b)\gamma.l.x^3 - \frac{1}{2^3.3} (a+b)\gamma.x^4 + \frac{1}{2^2} (a+b)\sigma_{tm}bx^2 - \frac{1}{2^3.3} (a+b)\gamma.l^3x - \frac{1}{2^2} (a+b)\sigma_{tm}b.lx + K_1 \right]$$

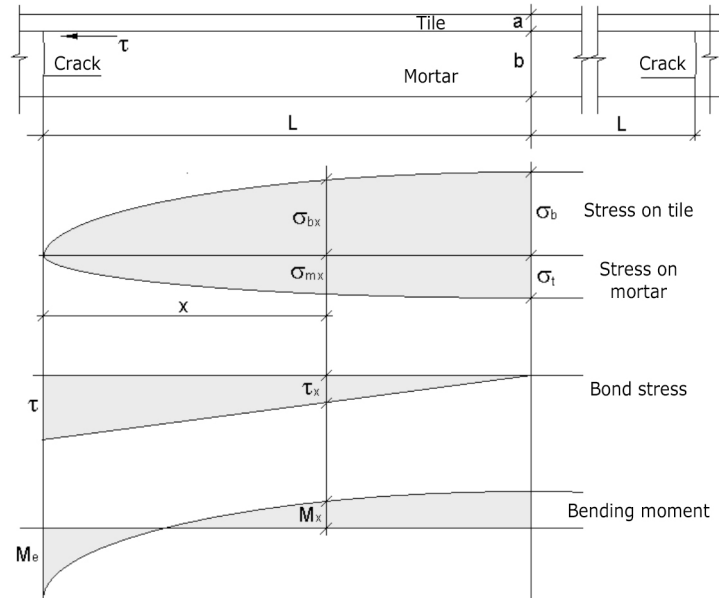
For  $x = 0$   $f = 0$  then  $K_1 = 0$

For  $x = l/2$ , deflection in the centre of the span:

$$f_x = \frac{1}{EI} \left[ \frac{5}{384} (a+b)\gamma.l^4 - \frac{1}{2^4} (a+b)\sigma_{tm}b.l^2 \right] \quad (A4)$$

### 3. DEDUCTION OF THE VALUE OF $M_e$ AND $\sigma_{bal}$ IN A FLOORING FRAGMENT

#### 3.1. INFLUENCE OF SHRINKAGE



*Scheme of the situation of the inter-crack stretch. Graph of stresses and moments.*

The function that represents the stress at each point is obtained from the integration of the stress function on the left of the section. Consequently, as the distribution of " $\tau_x$ " is a straight line with known slope and ordinate at the origin:

$$\tau_x = \frac{\tau}{L} x - \tau$$

The equilibrium of forces requires that throughout the mortar section:

$$\sigma_{mx} b = \int \tau_x dx = \int \left[ \frac{\tau}{L} x - \tau \right] dx = \frac{\tau}{2L} x^2 - \tau x + K$$

Since for  $x = 0$   $\sigma_m = 0$ :  $K = 0$

$$\sigma_{mx} b = \frac{\tau}{2L} x^2 - \tau x$$

A force, applied in the centre of the mortar that must be balanced by another in the tile of the same magnitude, applied in the centre of the tile.

The moment that they generate is the product of one of these forces by the arm or distance between the point of application of their resultants  $(a+b)/2$ :

$$M_x = \left[ \frac{\tau}{2L} x^2 - \tau x \right] \cdot \left[ \frac{a+b}{2} \right]$$

This is the function of moments considering the stretch without embedding at the ends.

The expression that measures the rotation in each section is:

$$\Phi_x = \frac{1}{EI} \int M x dx = \frac{1}{EI} \left[ \frac{a+b}{2} \right] \int \left[ \frac{\tau}{2L} x^2 - \tau x \right] dx$$

$$\Phi_x = \frac{1}{EI} \left[ \frac{a+b}{2} \right] \left[ \frac{\tau}{6L} x^3 - \frac{\tau}{2} x^2 + K_1 \right]$$

For  $x = L$   $\Phi = 0$

$$\Phi_L = \frac{1}{EI} \left[ \frac{a+b}{2} \right] \left[ \frac{\tau}{6L} L^3 - \frac{\tau}{2} L^2 + K_1 \right] = 0$$

$$\left[ \frac{\tau}{6L} L^3 - \frac{\tau}{2} L^2 + K_1 \right] = 0$$

$$K_1 = \frac{\tau}{3} L^2$$

$$\Phi_x = \frac{1}{EI} \left[ \frac{a+b}{2} \right] \left[ \frac{\tau}{6L} x^3 - \frac{\tau}{2} x^2 + \frac{\tau}{3} L^2 \right]$$

For  $x = 0$

$$\Phi_0 = \frac{1}{EI} \left[ \frac{a+b}{2} \right] \cdot \frac{\tau}{3} L^2$$

The rotation that imposes the moment of embedding at the end is:

$$\Phi_0 = \frac{Me \cdot 2L}{3EI} + \frac{Me \cdot 2L}{6EI} = \frac{Me \cdot L}{EI}$$

Setting equal

$$\frac{1}{EI} \left[ \frac{a+b}{2} \right] \cdot \frac{\tau}{3} L^2 = \frac{Me \cdot L}{EI}$$

$$\left[ \frac{a+b}{2} \right] \cdot \frac{\tau}{3} L^2 = Me \cdot L$$

$$Me = \frac{\tau}{3} L \left[ \frac{a+b}{2} \right]$$

Since  $\tau = \sigma \tau / \beta$

$$Me = \frac{\sigma_t}{3\beta} L \left[ \frac{a+b}{2} \right]$$

and  $L = 2 \beta b$

$$Me = \frac{2\sigma_t b}{3} \left[ \frac{a+b}{2} \right] \quad (A5)$$

As the tile section on top of the crack is subject to simple bending with a maximum stress of:

$$\sigma_{bal} = \frac{Me}{W_b} = \frac{6Me}{a^2}$$

The expression becomes:

$$\sigma_{bal1} = 2\sigma_r b \frac{a+b}{a^2} \quad (A6)$$

### 3.2. INFLUENCE OF THE OWN WEIGHT OF THE FRAGMENT

The action of the own weight can be calculated independently and be deducted from that determined by the shrinkage.

#### Influence of the own weight

The equation of moments considering a beam supported with a uniform load would be:

$$M_x = (a+b)\gamma Lx - (a+b)\gamma \frac{x^2}{2}$$

The function that determines the rotation:

$$\Phi_x = \frac{1}{EI} \int M x dx = \frac{1}{EI} \left[ (a+b)\gamma L \frac{x^2}{2} - (a+b)\gamma \frac{x^3}{6} + K \right]$$

For  $x = L$   $\Phi = 0$

$$(a+b)\gamma \frac{L^3}{2} - (a+b)\gamma \frac{L^3}{6} + K = 0$$

$$K = (a+b)\gamma \frac{L^3}{3}$$

Then

$$\Phi_x = \frac{1}{EI} \left[ (a+b)\gamma L \frac{x^2}{2} - (a+b)\gamma \frac{x^3}{6} + (a+b)\gamma \frac{L^3}{3} \right]$$

For  $x = 0$

$$\Phi_0 = \frac{1}{EI} (a+b)\gamma \frac{L^3}{3}$$

The rotation that imposes the moment of embedding at the end is:

$$\Phi_0 = \frac{Me \cdot L}{EI}$$

Setting equal

$$\frac{Me \cdot L}{EI} = \frac{1}{EI} (a + b) \cdot \gamma \frac{L^3}{3}$$

From which:

$$Me = (a + b) \cdot \gamma \frac{L^2}{3} \quad (A7)$$

The maximum stress in the tile corresponding to this action in the tile would be:

$$\sigma_{bal2} = \frac{6Me}{a^2} = \frac{2(a + b)}{a^2} \gamma \cdot L^2 \quad (A8)$$

### 3.3. COMPOSITION OF OPPOSITE STRESSES Owing TO THE TWO ACTIONS

The difference of opposite stresses owing to shrinkage and the own weight

$$\sigma_{bal} = 2\sigma_t b \frac{a + b}{a^2} - 2 \frac{a + b}{a^2} \gamma \cdot L^2$$

The difference would be:

$$\sigma_{bal} = 2 \frac{a + b}{a^2} (\sigma_t b - \gamma \cdot L^2)$$